D Meson Semileptonic and Leptonic Decays in $N_f = 2$ Lattice QCD

Richard Evans[*]

North Carolina State University
Department of Nuclear Engineering
Raleigh, NC, USA 27695
E-mail: rtevans@ncsu.edu

Gunnar Bali

Institut für Theoretische Physik, Universität Regensburg,
93040 Regensburg, Germany
E-mail: gunnar.bali@physik.uni-regensburg.de

Sara Collins

Institut für Theoretische Physik, Universität Regensburg,
93040 Regensburg, Germany
E-mail: sara.collins@physik.uni-regensburg.de

We present two separate but complementary analyses: a summary of our work on improved methods for D meson semileptonic form factor calculations, and a preliminary calculation of the D meson leptonic decay constants, f_D and f_{D_s}. This work is performed on the QCDSF configurations with $N_f = 2$ non-perturbatively improved Wilson fermions with pseudoscalar masses ranging from 170 to 380 MeV.

---

[*]Speaker.

1. Summary of Semileptonic Calculation Methods Studied

In this work, we study stochastic and sequential methods for calculating, $f_+(q^2)$ and $f_0(q^2)$, the form factors relevant for the semi-leptonic decays, $D \to \pi l \nu_l$ and $D \to K l \nu_l$. $f_+(q^2)$, together with perturbatively known factors can be used to extract CKM matrix elements from the experimental results for the differential decay rate. The form factors are extracted from the vector current matrix element, $\langle D(p_D)|V_\mu|\pi(p_\pi)\rangle$, which, on the lattice, is extracted from the three-point correlator,

$$C_3(T,t;\vec{p}_D,\vec{q}) = e^{-i\vec{p}_D\cdot\vec{x}+i\vec{q}\cdot\vec{y}}\left\langle M_u^{-1}(\vec{0},0;\vec{x},T))\gamma_5 M_c^{-1}(\vec{x},T;\vec{y},t)\gamma_\mu M_l^{-1}(\vec{y},t;\vec{0},0)\gamma_5 \right\rangle, \qquad (1.1)$$

where u, c, and l label the spectator-, heavy- (charm-like), and daughter-quark propagators M^{-1}. $C_3(T,t;\vec{p}_D,\vec{q})$ represents creating a pion at time 0, inserting the vector operator, $V_\mu = \bar{q}_u\gamma_\mu q_c$, with momentum transfer q at time t and destroying a D meson with momentum p_D at time T.

At first glance, eq. (1.1) presents a problem as C_3 requires the calculation of the "all-to-all" propagator, $M_c^{-1}(\vec{x},T;\vec{y},t)$, which is computationally too expensive to obtain. However, methods exist to calculate this propagator in combination with M_l^{-1} or alternatively to estimate M_c^{-1} stochastically. We compare the efficiencies of 3 different approaches to calculating C_3:

(a) The Sequential Propagator Method: this is the standard method currently used in calculations of this type. C_3 is computed by inverting the heavy-quark propagator M_c on a "Sequential Source", $\gamma_5 e^{i\vec{p}_D\cdot\vec{x}}M_u^{-1}(\vec{x},T;\vec{0},0)$,

$$G(\vec{y},t;\vec{p}_D,T;\vec{0},0) = \sum_{\vec{x}} M_c^{-1}(\vec{y},t;\vec{x},T)\gamma_5 e^{i\vec{p}_D\cdot\vec{x}}M_u^{-1}(\vec{x},T;\vec{0},0).$$

$G(\vec{y},t;\vec{p}_D,T;\vec{0},0)$ is combined with M_l^{-1} and the appropriate Γ matrices to arrive at eq. (1.1).

(b) The Stochastic Propagator Method: this approach utilizes $\mathbb{Z}_2$ noise vectors, $\eta^{[\ell]}, \ell = 1,\ldots,N$, with the property

$$\frac{1}{N}\sum_\ell \eta_i^{[\ell]}(x)\eta_j^{\dagger[\ell]}(z) = \delta_{xz}\delta_{ij} + \mathcal{O}(1/\sqrt{N}) \qquad (1.2)$$

can be used to compute the heavy-quark propagator directly, $\psi_c^{[\ell]}(\vec{y},t) = M_c^{-1}(\vec{y},t;\vec{z},T)\eta^{[\ell]}(\vec{z},T)$.

(c) The One-end Method [1]: this method combines the stochastic and sequential approaches. The same Z_2 noise vector is used to compute the heavy- and spectator-quark propagators,

$$\begin{aligned} \psi_c^{[\ell]}(\vec{y},t) &= M_c^{-1}(\vec{y},t;\vec{z},T)e^{i\vec{p}_D\cdot\vec{z}}\eta^{[\ell]}(\vec{z},T), \\ \psi_l^{[\ell]}(\vec{w},0) &= M_l^{-1}(\vec{w},0;\vec{x},T)\eta^{[\ell]}(\vec{x},T). \end{aligned} \qquad (1.3)$$

M_l^{-1} is then used as a sequential source (with the momentum and Γ factors) for the daughter product (u) solve.

The study, summarized below, is an extension of the initial work presented in Ref. [2]. Full details of the comparison of the three methods can be found in Ref. [3]. Following this, we present preliminary results for the decay constants f_{D_s} and f_D.
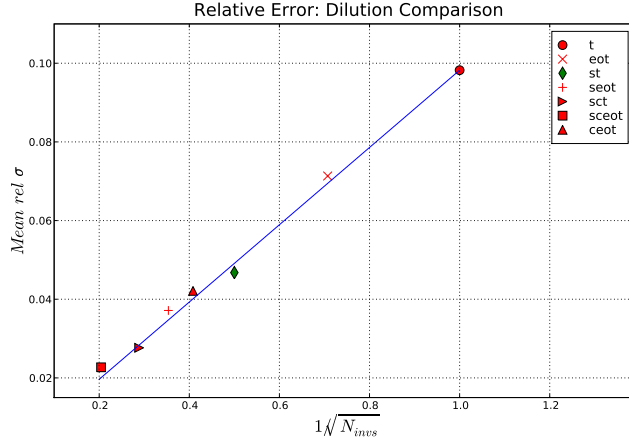
Figure 1: The relative error, averaged over the time slices, of $V_0(q_{max}^2)$ for 7 different combinations of even/odd (eo), spin (s), and color (c) partitioning as a function of the number of solves N_{invs} required to calculate the partitioned correlator from a single noise vector. All correlators are fully time (t) partitioned.

1.1 Comparison of Noise Reduction Techniques

We focused our efforts on minimizing the noise in the Stochastic Propagator Method, making the assumption that the same techniques are effective in the One-end Method. In the end, we found the most efficient noise reduction technique, simple time and spin partitioning [4], provides a similar noise reduction in both methods. Comparisons and tests were performed on two QCDSF ensembles with $N_f = 2$ non-perturbatively improved clover fermions and lattice spacings ~ 0.08 fm (see Ref. [3] for details). The behavior of the noise, which we quantify using the relative errors, σ, is comparable on both ensembles.

The following ratio of correlators was used for comparing noise reduction techniques,

$$V_0(q_{max}^2) = \frac{C_3(T,t;\vec{p}=0,\vec{q}=0)}{C_2^\pi(t)C_2^D(T-t)}, \tag{1.4}$$

where $\lim_{T\gg t\gg 0} V_0(q_{max}^2) \to \frac{1}{Z_\pi Z_D}\langle\pi(\vec{0})|V_0|D(\vec{0})\rangle$. This ratio is particularly convenient because it is the statistically cleanest correlator, with $\vec{p}_\pi = \vec{p}_D = 0$. By comparing the relative errors of $V_0(q_{max}^2)$ constructed with different combinations of time partitioning and the Hopping Parameter Acceleration [5] we determined that full time partitioning is crucial for efficient noise reduction and hence chose it as the basis of our partitioning scheme. Note that this does not increase our cost relative to the Sequential Propagator Method, because that method is also limited to using a single sink time-slice to construct correlators.

Starting from full time partitioning, we tried all combinations of spatial (even/odd), color, and spin partitioning, as shown in Fig. (1), for a single configuration with 100 noise vectors. The pion source is fixed at $t = 0$ and the D meson sink at $T = 24$ for all partitionings. The blue line represents the expected, purely statistical, decrease of the noise with increasing the number of full time partitioned vectors. Perhaps surprisingly, none of the alternative partitioning methods provide

	Computational Cost of the 3 Methods
1. Seq. Prop	$12(m_l)(W_{src})(C_l) + 12(m_u)(C_l) + 12(m_u)(\vec{p}_D)(W_{snk})(C_h)$
2. Z_2 Prop	$12(m_l)(W_{src})(C_l) + 12(m_u)(C_l) + 4N(C_h)$
3. One-end	$4N(\vec{p}_D)(W_{snk})(C_h) + 4N(m_u)(C_l) + 48N(m_u)(\vec{p}_\pi)(m_l)(W_{src})(C_l)$

Table 1: The approximate costs of the light-quark and heavy-quark solves are labels by C_l and C_h respectively, where $C_l \approx 30C_h$. The integer factors indicate the cost in inversions of a parameter combination. The parameters are: (W_{src}/W_{snk}) the number of source/sink smearings, ($\vec{p}_\pi/\vec{p}_D$) the number of π/D momenta, and (m_u/m_l) the number of daughter/spectator quark masses.

significant improvement over exclusively using full time dilution: spin partitioning on its own appears to have smaller errors, although the effect is small. This result is consistent over the other configurations we examined, causing us to choose full time and spin partitioning as our preferred variance reduction technique.

1.2 Cost Comparison Summary

The computational costs of these three methods are summarized in Table 1. Essentially, the Stochastic Propagator Method offers greater flexibility than the Sequential Propagator Method, but introduces stochastic noise that must be reduced. However, the greater flexibility in this method allows correlators with all combinations of momenta to be generated with a fixed number of quark inversions. These additional correlators are advantageous in two ways: additional correlators at each q^2 are available for averaging, and additional q^2 data points are available to aid in the $q^2 \to 0$ extrapolations. The One-end Method is less flexible than the Stochastic Propagator Method, but could have greatly reduced statistical errors due to an additional volume average arising in the correlators.

Data which are representative of the noise behavior are shown in Fig. (2) for q^2_{max}; correlators at additional q^2 were also examined and seen to have similar behavior. A simple comparison of the errors shown in this figure, along with consideration for the computational costs, suggests that the One-end method is not competitive with the other two methods.

In Ref. [3] an extensive analysis of the relative efficiencies of the Sequential and Stochastic propagator methods is presented. It is seen that the additional rotationally equivalent correlators available at fixed cost in the Stochastic approach results in an overall reduction of statistical errors and a net gain in efficiency.

1.3 Matching and Results for the Form Factors

In order to connect our results to observables of phenomenological interest we perform the matching and $\mathcal{O}(a)$ improvement of the vector current. The matching calculation takes the form,

$$V_\mu^{\text{cont}}(q^2) = Z_V \left[V_\mu(q^2) + aic_V \partial_\nu T_{\mu\nu}(q^2) \right] , \tag{1.5}$$

where $T_{\mu\nu} = \bar{\psi}_c \sigma_{\mu\nu} \psi_l$ is the tensor current with $\sigma_{\mu\nu} = \frac{i}{2}[\gamma_\mu, \gamma_\nu]$. The matching factor Z_V is known non-perturbatively [6], while the coefficient of the improvement term, c_V, is known to one-loop in

4
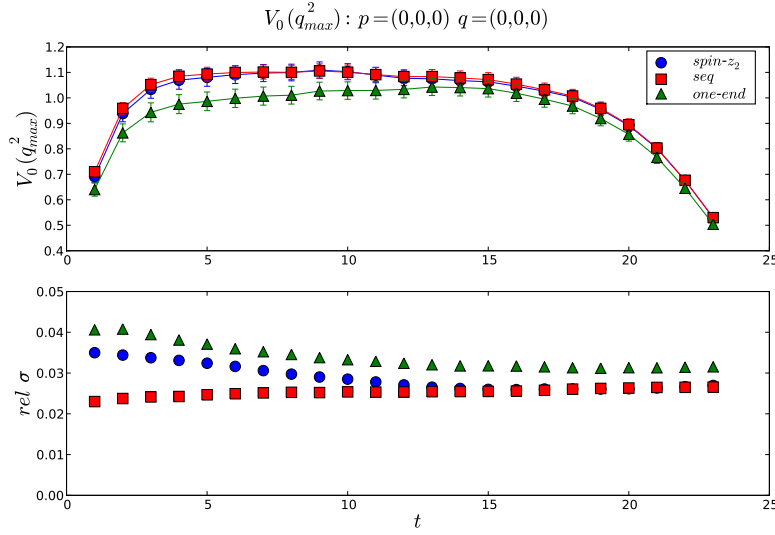
Figure 2: The upper plot shows $V_0(q_{max}^2)$ generated with the Sequential Method (red squares), the Stochastic Method (blue circles) and the One-end Method (green triangles). The lower plot shows the relative errors of each time-slice. 250 configurations were used.

$m_{\pi,sea}$	Volume	N_{cfgs}
~ 380 MeV	$24^3 \times 48$	393
~ 270 MeV	$24^3 \times 48$	348
~ 170 MeV	$40^3 \times 64$	336

Table 2: Lattice spacing is ~ 0.08 fm on all ensembles. 4 time sources per configuration have been used on the $m_{\pi,sea} = 170$ MeV and $m_{\pi,sea} = 270$ MeV ensembles. One time source, with random location, was used for the $m_{\pi,sea} = 380$ MeV ensemble.

perturbation theory [7]. The form factors extracted from the corresponding matrix element, $\langle V_\mu^{\text{cont}} \rangle$ are shown in Fig. (3) for the $N_f = 2$ ensemble with $m_{\pi,sea} = 270$ MeV. 24 spin-partitioned stochastic sources were used (i.e. 96 inversions).

We extract $f_0(0) = f_+(0)$ using the *BK* parametrization for the $q^2 \to 0$ interpolation [9]:

$$f_0(q^2) = \frac{c}{1 - \tilde{q}^2/\beta}, \quad f_+(q^2) = \frac{c}{(1 - \tilde{q}^2)(1 - \alpha\tilde{q}^2)}, \tag{1.6}$$

where $\tilde{q} = q/m_D^*$ and m_D^* is the vector D meson mass. The result for $f_+(0) = 0.593(19)$ is comparable to previous determinations. The error shown is statistical only. We also investigated extracting the form factor from the scalar matrix element, following the method of Ref. [8]. Consistent results with slightly larger statistical errors were obtained.

2. Preliminary Results for the Decay Constants f_D and f_{D_s}

In this section we present the calculation of the leptonic decay constants f_D and f_{D_s} using the
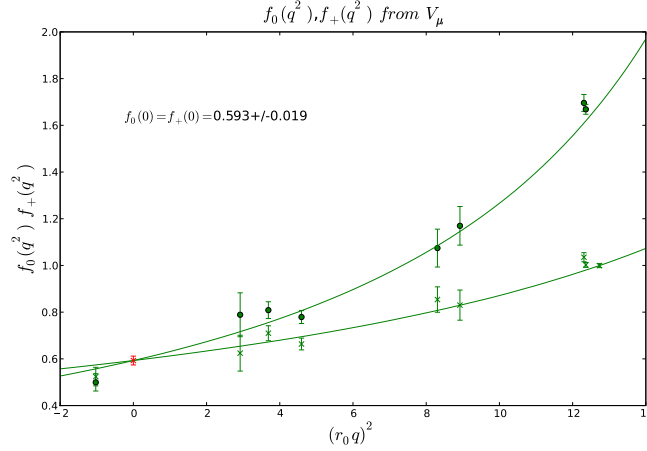
Figure 3: Results using the Stochastic Propagator Method with 24 ($\times$4 spin partitioned) stochastic vectors and 539 configurations $\times$ 4 time sources.

three ensembles shown in Table 2. The decay constants are defined in terms of the axial-vector matrix element, $\langle 0|A_\mu|D_q\rangle = ip_\mu f_{D_q}$, where to $\mathcal{O}(a^2)$ on the lattice,

$$A_\mu^{cont.} = Z_A \left[1 + \frac{1}{2}ab_A(m_c + m_l)\right] \left[A_\mu + aic_A\partial_\mu P\right] \tag{2.1}$$

Z_A and and c_A are known non-perturbatively [6] and b_A to one-loop [7]. We extract the heavy-light decay constant for light quark masses around the strange quark mass and lighter. We then perform a chiral interpolation/extrapolation using the continuum, partially quenched, NNLO HMχPT expression derived in Ref. [10],

$$f_D\sqrt{M_D} = \beta(1 + \omega\{chiral\,logarithms\} + \alpha_v^0 m_{\pi,val}^2 + \alpha_s^0 m_{\pi,sea}^2 + \alpha_v^1 m_{\pi,val}^4 + \alpha_s^1 m_{\pi,sea}^4), \tag{2.2}$$

to obtain f_D and f_{D_s}. However, we found our fits and extrapolations to be insensitive to the chiral logarithms. At this point only a single lattice spacing, $a \sim 0.08$ fm was used. Therefore our discretization errors are currently unknown, although naively they are of order $\mathcal{O}(a^2m_c^2)$. The fit and extrapolation result, neglecting chiral logarithms, are presented in Fig. (4). The errors shown in the figure are statistical only.

3. Outlook

Our study of semi-leptonic form factors has shown the Stochastic Method is flexible and cost-effective: a wider range of momenta with reasonable statistics are obtained through averaging of equivalent momenta compared to using the Sequential Method. We found that time partitioning is the only beneficial variance reduction technique of those tested. We intend to exploit the Stochastic Method further by studying decay involving radial excitations and decays to flavour singlet states.

Acknowledgments
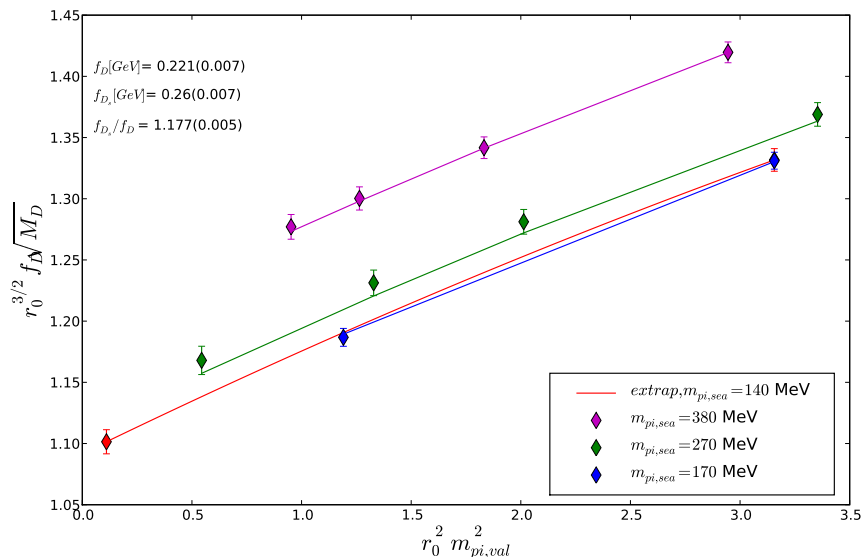
Figure 4: The chiral extrapolation and preliminary values for f_D and f_{D_s} in terms of $r_0 = 0.467$ fm, as determined in Ref. [11].

(Stifterband für die Deutsche Wissenschaft). Computations were performed on Regensburg's Athene HPC cluster and the SGI ICE 8200 at HLRN (Berlin-Hannover, Germany). The Chroma software suite [12] was used extensively in this work.

References

[1] C. McNeile and C. Michael [UKQCD Collaboration], Phys. Lett. B **556** (2003) 177 [arXiv:hep-lat/0212020].

[2] R. Evans, G. Bali, S. Collins, PoS **LAT2009**, (2009) 244. [arXiv:0911.3254 [hep-lat]].

[3] R. Evans, G. Bali and S. Collins, Phys. Rev. D **82**, (2010) 094501 [arXiv:1008.3293 [hep-lat]].

[4] S. Bernardson, P. McCarty and C. Thron, *Comput. Phys. Commun.* **78**, (1993) 256.

[5] C. Thron, S. J. Dong, K. F. Liu and H. P. Ying, Phys. Rev. D **57** (1998) 1642 [arXiv:hep-lat/9707001].

[6] M. Göckeler, R. Horsley, Y. Nakamura *et al.*, Phys. Rev. **D82** (2010) 114511. [arXiv:1003.5756 [hep-lat]].

[7] S. Sint and P. Weisz, *Nucl. Phys.* B **502** (1997) 251 [arXiv:hep-lat/9704001].

[8] H. Na, C. T. H. Davies, E. Follana *et al.*, PoS **LAT2009** (2009) 247. [arXiv:0910.3919 [hep-lat]].

[9] D. Becirevic and A. B. Kaidalov, Phys. Lett. B **478** (2000) 417 [arXiv:hep-ph/9904490].

[10] S. R. Sharpe and Y. Zhang, Phys. Rev. D **53** (1996) 5125 [arXiv:hep-lat/9510037].

[11] M. Göckeler *et al.* [QCDSF and UKQCD Collaborations], Nucl. Phys. B **812**, (2009) 205 [arXiv:0810.3762 [hep-lat]].

[12] R. G. Edwards and B. Joo [SciDAC, LHP and UKQCD Collaborations], *The Chroma software system for lattice QCD, Nucl. Phys. Proc. Suppl.* **140** (2005) 832 [arXiv:hep-lat/0409003].